

# Normalizing Flows are Capable Visuomotor Policy Learning Models

Simon Kristoffersson Lind<sup>\*1</sup>

Jialong Li\*

Maj Stenmark

Volker Krüger

Preprint

**Abstract**—The field of general purpose robotics has recently embraced powerful probabilistic models, such as diffusion models, to model and learn complex behaviors. However, these models often come with significant trade-offs, namely high computational costs for inference and a fundamental inability to quantify output uncertainty. We argue that a model’s trustworthiness, a critical factor for reliable, general-purpose robotics, is inherently linked to its ability to provide confidence measures.

In this work, we introduce Normalizing Flows Policy, a novel visuomotor policy learning model based on Normalizing Flows. We show that Normalizing Flows are a natural and powerful alternative to diffusion models, providing both a statistically sound measure of confidence and a highly efficient inference process. Through comprehensive experiments across four distinct simulated robotic tasks, we demonstrate that Normalizing Flows Policy achieves performance comparable to, and often surpassing, Diffusion Policy, and it does so not only with improved sample efficiency but also with up to 30 times faster inference. Additionally, our ablation study validates several key architectural and training techniques that enable Normalizing Flows to perform well in this domain.

## I. INTRODUCTION

Diffusion Policy (DP) [1] is one of the mainstream methods for visuomotor policy learning using a Denoising Diffusion Probabilistic Model (DDPM) [2]. This approach has secured a place in robot policy learning due to its powerful expressive capabilities.

Despite impressive performance in modeling robotic behaviors, diffusion models exhibit a number of drawbacks. Most importantly, they do not produce any measure of confidence or uncertainty in their outputs. An implication of this is that diffusion models cannot give any guarantees regarding the quality of their outputs, which is a weakness.

- First and foremost, uncertainty is inevitable in general-purpose robotics, and we argue that a measure of confidence is necessary for a model to be considered trustworthy. Crucially, the model should be able to use this confidence to improve the generated action sequences.
- Additionally, the training and inference costs for diffusion policy are often substantial, primarily because of the sequential denoising steps required for action generation.

With this work, we propose to use Normalizing Flows (NFs) [3] for visuomotor policy learning. We argue that NFs are a natural alternative to diffusion models, possessing

neither of the aforementioned flaws. NFs provide a measure of confidence for their outputs through a statistically sound approximation to the underlying probability. Additionally, inference in an NFs requires only a single pass through the model, which makes inference much more efficient. While providing an output probability, and fast inference, NFs also exhibit the same properties that make diffusion models desirable, namely stochastic generative sampling, and the ability to model complex and multimodal distributions. Through experiments within the RoboTwin 2.0 simulation framework [4], we show that NFs are able to learn robotic tasks with a success rate comparable to, and often better than, DP, especially when training data is sparse.

To summarize, our contributions are as follows:

- We propose to use NFs for visuomotor policy learning and introduce our model, Normalizing Flow Policy (NF-P).
- Through experiments with 4 different simulated robotic tasks of varying difficulty, we show that NF-P reaches comparable performance to DP, and provides superior performance compared to DP when little training data is available.
- We demonstrate that NFs can provide an order of magnitude faster inference times compared to diffusion models.
- We validate several key techniques on normalizing flows to achieve strong performance in Visuomotor Policy Learning: visual and action conditioning, action-sequence based generation with stride, and likelihood optimization of the output.
- In an ablation study, we highlight various factors and design choices that affect the performance of NFs for visuomotor policy learning.

## II. RELATED WORK

### A. Visuomotor Policy Learning Models

Thanks to the accessibility and high information content of visual data, vision-based robot policy learning is a popular approach for learning from demonstrations. The simplest way under this paradigm is a direct regression or autoregression from the robot’s state or visual observations to the continuous actions to be executed [5] [6] [7] [8]. These models often adopt transformer-based architectures for scalability, and their inference is computationally efficient and reasonably fast due to a single-pass feed-forward process. However, they face challenges in modeling multimodal behaviors [9] and often lack well-explained mechanisms for extending to common downstream tasks in robotics, such as failure recovery.

<sup>\*</sup>Equal Contribution

<sup>1</sup>Corresponding author: simon.kristoffersson\_lind@cs.lth.se

All authors with Department of Computer Science, Lund University LTH, Lund, Sweden, [firstname.lastname@cs.lth.se](mailto:firstname.lastname@cs.lth.se)

## B. Diffusion-based policy learning

Compared to transformer-based regression and autoregressive models, the main difference with diffusion models is that they attempt to learn a distribution conditioned on visual observations and robot states, and then sample from this learned distribution using a multi-step diffusion process. Based on this, diffusion policy models have demonstrated strong capabilities in modeling multimodal behaviors and are easily extended to various action spaces [1]. Furthermore, the inherent expressive power of diffusion models sets them apart. However, precisely because of these characteristics, diffusion models also suffer from slow inference speeds and interpretability issues.

Many subsequent works on diffusion policy models have attempted to either expand on their existing strengths or compensate for their shortcomings. In terms of expansion, Hierarchical Diffusion Policy [10] combines a high-level diffusion model for planning with a low-level policy for execution, with the aim of improving performance on long-horizon tasks. Causal diffusion policy[11] integrates the temporal modeling of a causal transformer with the generative capabilities of a diffusion model to enhance the robustness of the generated results.

Regarding the drawbacks, one-step diffusion policy [12] aims to distill diffusion policy models and align the distillation using the KL divergence. The goal is to create a model that retains the performance of diffusion policies but generates results with a single-step sampling process. Although the distilled models do achieve higher sampling efficiency, their performance is generally on par with the original diffusion models. Another work, 3D Diffusion Policy [13], uses 3D point cloud as input, and preprocesses 3D point cloud inputs by cropping them to reduce task learning difficulty and significantly lowers the model size to ensure computational efficiency. However, a major challenge in this work is the data type itself; the acquisition and processing of point clouds require far more computation than images, making the overall pipeline difficult to describe as light. Additionally, RTI-DP [14] introduces a real-time iteration that also aim to improve real time pridiction of Diffusion Policy. Overall, similar to autoregressive models, policy models in the diffusion family have also inherited the low interpretability characteristic of diffusion models. Generally, during the inference process of a diffusion model, the final outcome is not easy to fully predict until the denoising process is complete.

Another recent addition is that of flow matching based Vision Language Action models, for example  $\pi_0$  [15] and  $\pi_{0.5}$  [16], which use large pretrained Vision Language Models to condition robotic action generation. While these models show impressive performance across various tasks, we refrain from comparison in our work due to the large amounts of pretraining required, and the sheer size of the underlying Vision Language Model.

## C. Normalizing Flows

Normalizing flows are well-known for their ability to compute data likelihoods and perform density estimation [17]. Their application in generative tasks has received decreasing attention in recent years, primarily due to the widespread belief that they have limited expressive power. However, recent work has validated the feasibility of normalizing flow models for image generation tasks [18], and tested the effectiveness of this method in behavior cloning [19], thereby revealing its potential for visuomotor policy learning.

Pioneering NFs architectures like RealNVP [17] and GLOW [20] use NFs to generate realistic images, highlighting their ability to learn and model complex and multimodal probability distributions. Additionally, our previous work [21], [22] uses NFs for out-of-distribution detection to create robust, adaptable robotic behaviors, which highlights NFs' ability to directly model probability densities.

## III. BACKGROUND

### A. Visuomotor Policy Learning

In its simplest form, visuomotor policy learning can be expressed as a supervised learning problem consisting of observation-action pairs  $(\mathbf{o}_t, \mathbf{a}_t)$ , in which the goal is to predict the action  $\mathbf{a}_t$  given the input observation  $\mathbf{o}_t$  at time  $t$ . However, robotic tasks are often multimodal, meaning that there are multiple, equally correct, possible action sequences from any state. As such, it is suitable to instead model policy learning as a generative problem, where the goal is to model  $p(\mathbf{a}_t|\mathbf{o}_t)$ , which is the approach adopted by for example Diffusion Policy [1].

### B. Diffusion Models

Diffusion models learn to generate samples from a given distribution  $p(\mathbf{x})$  by emulating a diffusion process in which a sample  $\mathbf{x}$  is gradually distorted until it is indistinguishable from noise. Sample generation is done by training a model to reverse the aforementioned diffusion process. While there exists several different methods of encoding and learning the reverse diffusion process, the most widely used is that of DDPM [2], which represents the diffusion process as a Markov chain, in which a clean data sample  $\mathbf{x}_0$  is iteratively perturbed by Gaussian noise:

$$p(\mathbf{x}_i|\mathbf{x}_{i-1}) = \mathcal{N}(\sqrt{\alpha_i}\mathbf{x}_{i-1}, (1-\alpha_i)\mathbf{I})$$

or equivalently:

$$p(\mathbf{x}_i|\mathbf{x}_0) = \mathcal{N}(\sqrt{\bar{\alpha}_i}\mathbf{x}_0, (1-\bar{\alpha}_i)\mathbf{I}), \quad \bar{\alpha}_i = \prod_{s=1}^i \alpha_s .$$

Here,  $\alpha_i$  is called the *noise schedule*, and controls how quickly or slowly the process converges to Gaussian noise.

With this Markov chain in place, the goal is to learn the reverse Markov chain:

$$p_{\theta}(\mathbf{x}_{i-1}|\mathbf{x}_i) = \mathcal{N}(\mu_{\theta}(\mathbf{x}_i, i), \Sigma_{\theta}(\mathbf{x}_i, i)) .$$

This is typically done by reparameterizing the diffusion process as:

$$\mathbf{x}_i = \sqrt{\bar{\alpha}_i} \mathbf{x}_0 + (1 - \bar{\alpha}_i) \epsilon, \quad \epsilon \sim \mathcal{N}(\mathbf{0}, \mathbf{I})$$

and then learning  $\epsilon_\theta(\mathbf{x}_i, i)$  to minimize the  $L_2$ -loss

$$\|\epsilon - \epsilon_\theta(\mathbf{x}_i, i)\|$$

Sampling is then performed by sampling Gaussian noise  $\mathbf{x}_N \sim \mathcal{N}(\mathbf{0}, \mathbf{I})$ , and iteratively removing noise, until a clean sample  $\mathbf{x}_0$  is recovered:

$$\mathbf{x}_{i-1} = \frac{1}{\sqrt{\bar{\alpha}_i}} \left( \mathbf{x}_i - \frac{(1 - \bar{\alpha}_i)^2}{\sqrt{1 - \bar{\alpha}_i}} \epsilon_\theta(\mathbf{x}_i, i) \right) + \sigma_i^2 \epsilon .$$

Various formulas exist for setting  $\sigma_i$ . A common choice, initially proposed in DDIM [23], is to set  $\sigma_i = 0$ , which makes the generating procedure deterministic.

Naturally, generating a sample by iteratively applying the learned model  $\epsilon_\theta$  is a time-consuming process. DDIM addresses this issue by reformulating the generating process as  $p_\theta(\mathbf{x}_{i-1} | \mathbf{x}_i, \mathbf{x}_0)$ . While this may seem counter-intuitive, since  $\mathbf{x}_0$  is unknown when generating samples, it effectively decouples the diffusion and denoising processes, which in turn allows the generating process to use a different number of steps compared to the diffusion process. In DDIM, generation is performed by predicting  $\mathbf{x}_0$  directly:

$$f_\theta(\mathbf{x}_i) = \frac{\mathbf{x}_i - \sqrt{1 - \bar{\alpha}_i} \epsilon_\theta(\mathbf{x}_i, i)}{\sqrt{\bar{\alpha}_i}} .$$

This prediction is then used to compute  $\mathbf{x}_{i-1}$ :

$$\mathbf{x}_{i-1} = \sqrt{\bar{\alpha}_{i-1}} f_\theta(\mathbf{x}_i) + \sqrt{1 - \bar{\alpha}_{i-1} - \sigma_i^2} \epsilon_\theta(\mathbf{x}_i, i) + \sigma_i \epsilon .$$

Note that this formulation allows for any index  $\mathbf{x}_{i-k}$ , given  $0 \leq i - k < i$ .

A conditional action distribution  $p_\theta(\mathbf{x}_0 | C)$  can be modeled by adding the condition into  $\epsilon_\theta(\mathbf{x}_i, i, C)$ , as is the case in Diffusion Policy [1].

### C. Normalizing Flows

Similarly to diffusion models, normalizing flows also learn to model a distribution  $p(\mathbf{x})$  by transforming clean samples into Gaussian noise, though the method of this transformation is different. Instead of modeling a diffusion process, normalizing flows represent the entire transformation as a single function [3]:

$$\mathbf{u} = T(\mathbf{x}), \quad \mathbf{x} \sim p(\mathbf{x}), \quad \mathbf{u} \sim p_u(\mathbf{u}) . \quad (1)$$

It should be noted that  $p_u$  can be chosen freely, but the most common choice is Gaussian noise  $p_u = \mathcal{N}(\mathbf{0}, \mathbf{I})$ . Importantly,  $T$  is a *diffeomorphism*, which means that it is bijective with both  $T$  and  $T^{-1}$  being differentiable. Naturally, the bijective property allows sampling by:

$$\mathbf{x} = T^{-1}(\mathbf{u}), \quad \mathbf{u} \sim p_u(\mathbf{u}) .$$

Additionally, both  $T$  and  $T^{-1}$  being differentiable enables direct computation of  $p(\mathbf{x})$ :

$$p(\mathbf{x}) = p_u(T(\mathbf{x})) |\det J_T(\mathbf{x})| . \quad (2)$$

Here,  $J_T(\mathbf{x})$  refers to the Jacobian matrix of  $T(\mathbf{x})$ .

Constructing a  $T$  that fulfills (1) for any distribution  $p(\mathbf{x})$  is non-trivial, and as such learning-based methods, usually neural networks, are the only viable option. The primary challenge in normalizing flows is to design a neural network-based  $T$  that is sufficiently expressive, while fulfilling the requirements for a diffeomorphism in addition to having a tractable Jacobian determinant.

A common way to design  $T$ , pioneered by RealNVP [17], is *coupling layers*. Coupling layers first divide their input  $\mathbf{x} = [x_1, x_2, \dots, x_D]$  into two parts, commonly:

$$\mathbf{x}_1 = [x_1, \dots, x_{D/2}], \quad \mathbf{x}_2 = [x_{D/2+1}, \dots, x_D] .$$

$\mathbf{x}_1$  is then transformed using an invertible and differentiable function  $f_\theta(\mathbf{x}_1)$ , with parameters  $\theta$  computed from  $\mathbf{x}_2$ . Formally:

$$\begin{aligned} \mathbf{x}'_1 &= f_\theta(\mathbf{x}_1), \quad \theta = \text{NN}(\mathbf{x}_2) \\ \mathbf{x}' &= \text{concat}(\mathbf{x}'_1, \mathbf{x}_2) . \end{aligned} \quad (3)$$

In this formulation, NN has no restrictions, and is usually a regular feed-forward neural network. Various choices exist for the design of  $f_\theta$ , arguably the most common being an element-wise linear transform:

$$f_\theta(\mathbf{x}_1) = \mathbf{x}_1 \cdot \alpha + \beta, \quad \text{with } (\alpha, \beta) = \theta .$$

In this work, however, we adopt Neural Spline Flows [24], which constructs  $f_\theta$  as a rational-quadratic spline.

## IV. METHODOLOGY

In this section, we discuss our design choices for the NF-P model.

### A. Observation encoding and conditioning

A pre-trained ResNet18 [25] is used to extract an embedding vector from each image before it is passed to the backbone. This image embedding is supplemented with a vector representing the latest action, and these together form our observation  $\mathbf{o}_t$ . Similarly to diffusion models, a conditional distribution can be modeled by adding a fixed conditioning vector to the NN function in the formulation (3) as  $\theta = \text{NN}(\mathbf{x}, \mathbf{o}_t)$ .

### B. Action Sequence Prediction with Stride

Since robotic tasks form a sequence of observation-action pairs  $(\mathbf{o}_0, \mathbf{a}_0), \dots, (\mathbf{o}_t, \mathbf{a}_t)$ , predicting a single action from a single state at a time can cause erratic, discontinuous motions. Additionally, stalling can easily occur when the difference between consecutive actions is small. Therefore, it is generally advantageous to instead operate on a sliding window of states and actions, which leads to more cohesive action sequences and reduced stalling [1]. Similar to DP, we design NF-P to operate on sequences for both observations and actions. As a result, the target distribution is instead formulated as  $p(\mathbf{a}_{t:t+n} | \mathbf{o}_{t-m:t})$ , where we use the shorthand  $\mathbf{o}_{i:j}$  to denote several time steps  $\mathbf{o}_i, \mathbf{o}_{i+1}, \dots, \mathbf{o}_j$ .

In addition, during our early testing, we observed that the normalizing flow model seems prone to stalling, even when

predicting a sequence of actions. To mitigate this issue, we introduce a stride along the temporal dimension for both the input observation sequences and action sequences during training. Specifically, during training, instead of learning the distribution

$$p(\mathbf{a}_t, \mathbf{a}_{t+1}, \dots, \mathbf{a}_{t+7} | \mathbf{o}_t, \mathbf{o}_{t-1}, \dots, \mathbf{o}_{t-3}) ,$$

we apply a stride  $s$ , and learn:

$$p(\mathbf{a}_t, \mathbf{a}_{t+s}, \dots, \mathbf{a}_{t+7s} | \mathbf{o}_t, \mathbf{o}_{t-s}, \dots, \mathbf{o}_{t-3s}) .$$

### C. Likelihood-based output optimization

In addition to being prone to stalling, our initial tests also revealed a tendency to produce large, erratic motions, which we believe stems from sampling low-probability regions within the action distribution. Based on this hypothesis, we leverage the NF's ability to evaluate  $p(\mathbf{a}|\mathbf{o})$ , and design NF-P to generate only high-probability actions by maximizing  $p(\mathbf{a}|\mathbf{o})$ . It is important to note that we do not wish to perform a full optimization procedure with the goal of finding a true global or local maximum of  $p(\mathbf{a}, \mathbf{o})$ , as we aim to preserve the generalizing effects of stochastic sampling. With this goal in mind, we apply two different techniques for guiding our sampling to high-probability actions:

- 10 steps of gradient ascent using Adam [26] with learn rate=0.1 starting from our initial sample.
- Generating a batch of 128 actions and selecting the one with highest probability.

In our experiments we denote these versions as NF-P<sub>opt</sub> and NF-P<sub>multi</sub> respectively.

Additionally, since NFs samples are created by first sampling  $\mathbf{u} \sim \mathcal{N}(\mathbf{0}, \mathbf{I})$ , we experiment with instead sampling  $\mathbf{u} \sim \mathcal{N}(\mathbf{0}, \sigma \mathbf{I})$ . Setting  $\sigma < 1$  should help guide our sampling towards higher-probability regions.

## V. EXPERIMENTS AND RESULTS

### A. Comparison between Diffusion Policy and Normalizing Flows Policy

In this section, we use the RoboTwin 2.0 [4] simulation environment to compare the performance of DP and our proposed NF-P. RoboTwin 2.0 is a scalable simulation framework that is capable of generating large amounts of data and testing in randomized simulations, effectively benchmarking the robustness and generalization of robotic policies, which is also used by other works [27] [28] [29].

1) *Diffusion Policy*: For the diffusion policy model we used as a comparison, we adopted the CNN-based version and aligned other settings with the DiffusionPolicy-C configuration from their work [1] based on the implementation provided with RoboTwin2.0 [4].

2) *Normalizing Flow Policy*: For our NF-P architecture, we use 10 Neural Spline Flow coupling layers, operating on alternating halves of the input vector. Parameters in the rational-quadratic splines are computed using a three-layer feed-forward neural network, with a hidden layer size of 2048 and a separate output head for each parameter.

We train NF-P to model a sliding window of 8 consecutive actions, given a sliding window of 4 observations. Like DP, we do not generate a new action sequence at each time step. Instead we execute 4 actions out of the 8 in each generated action sequence.

Regardless of the number of training episodes, we use the same training procedure. We use the Adam [26] optimizer with a fixed learn rate =  $10^{-4}$ , and train for 100 epochs with a batch size of 128, followed by 100 epochs with batch size 256, and finally another 100 epochs with batch size 512.

Our comparison with DP is performed with  $s = 4$ ,  $\sigma = 0.5$  for both NF-P<sub>opt</sub> and NF-P<sub>multi</sub>. The settings  $s = 4$  and  $\sigma = 0.5$  are validated in our ablation study.

3) *Evaluation with RoboTwin*: For our evaluation, we simulate the Aloha-AgileX robot with 4 different tasks of varying difficulty, and varying degrees of bi-manual collaboration:

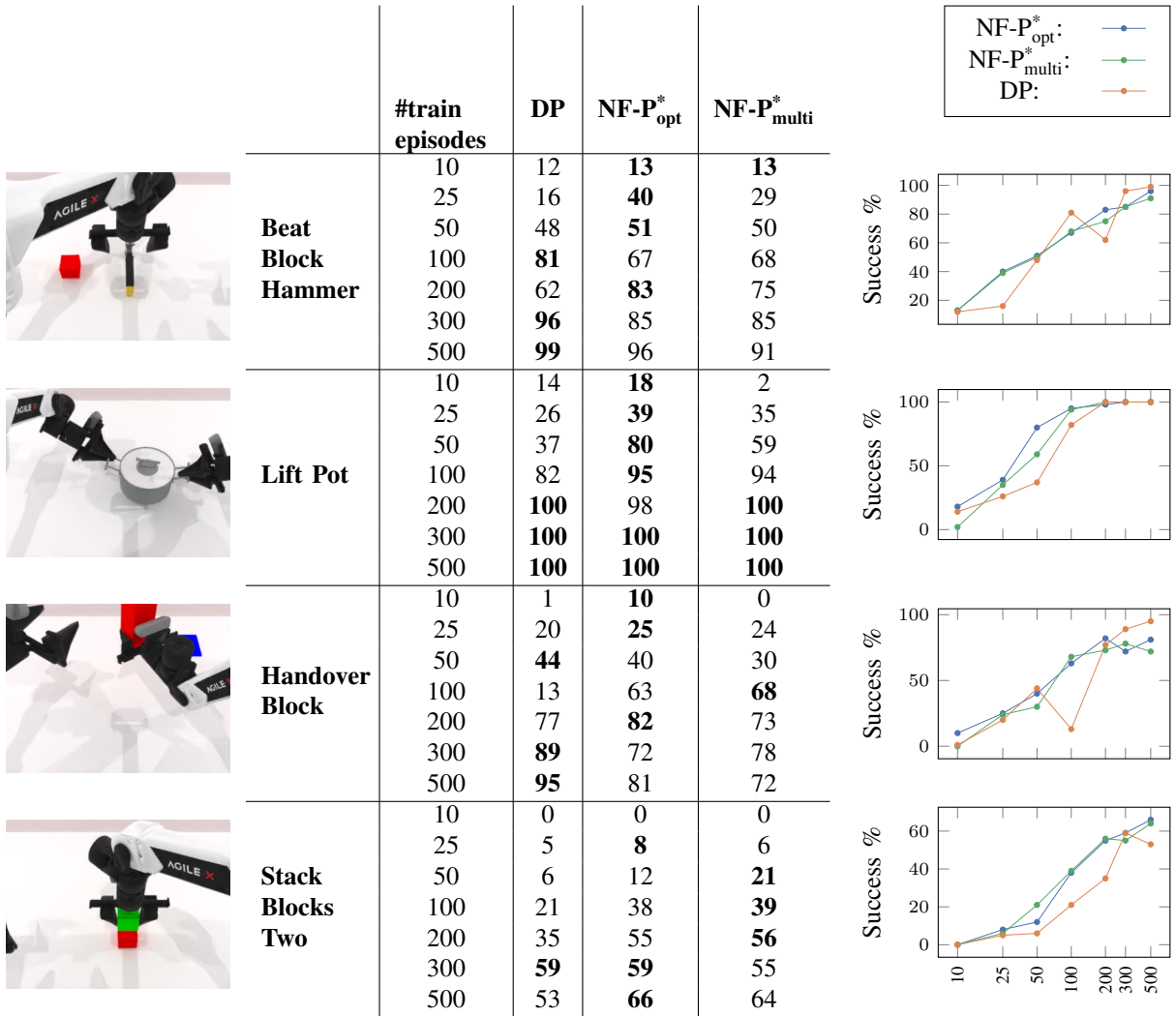
- **Beat Block Hammer**: Pick up a hammer and use it to "hammer" a colored cube.  
*Estimated difficulty*: Medium.  
*Randomized elements*: Position of hammer and cube.  
*Bi-manual elements*: Determine which arm can reach both the hammer and cube.
- **Lift Pot**: Lift a pot with two handles.  
*Estimated difficulty*: Easy.  
*Randomized elements*: Position of the pot.  
*Bi-manual elements*: Simultaneous lifting motion. Both arms have to grab one handle each.
- **Handover Block**: Pick up a colored cube, transfer it to the other arm, and place it in a marked goal location.  
*Estimated difficulty*: Hard.  
*Randomized elements*: Position of cube and goal.  
*Bi-manual elements*: Transfer cube between arms.
- **Stack Blocks Two**: Pick up one red and one green cube, and stack the green on top of the red cube.  
*Estimated difficulty*: Hard.  
*Randomized elements*: Positions of both cubes.  
*Bi-manual elements*: One cube per arm, and determine which arm should place first.

We believe these tasks are sufficient to get a comprehensive overview of how well NFs adapt to various scenarios.

Since one of the main concerns regarding NFs is their potentially limited expressive power, we are also interested in evaluating how NFs scale with varying amounts of training data. General perception is that diffusion models will exhibit better scaling properties as the amount of training data increases. For each of our selected robotic tasks, we train separate instances of each model using 10, 25, 50, 100, 200, 300, and 500 episodes of training data.

4) *Results*: Figure 1 shows the performance of DP, NF-P<sub>opt</sub>, and NF-P<sub>multi</sub> based on 100 randomized trial runs for each task. Performance is shown both in table and graph form. Inference times for DP and our different configurations of NF-P are shown in Table I.

5) *Discussion*: Looking at both the table and the graphs in Figure 1, it is immediately clear that both our NF-P variants



<sup>\*</sup>: Ours

Fig. 1. Evaluation results on 4 RoboTwin2.0[4] from 100 trials. **Left:** Figures indicate the setup of different tasks. **Middle:** Table shows the number of demonstrations used for each model and the corresponding success rates. **Right:** The change of success rate in the line chart.

TABLE I  
INFERENCE TIMES FOR DP VS. NF-P ON AN NVIDIA A100 40GB.

Model	Inference time (ms)
DP	701
NF-P	18
NF-P <sub>multi</sub> (batch=128)	19
NF-P <sub>opt</sub> (10 steps)	455

perform competitively with DP, even beating it in 17 out of our 28 test cases.

Perhaps the most interesting observation, that originates in the graphs of Figure 1, is that both models converge to high success rates with nearly identical trends as the number of training episodes increases. NF-P maintains competitive performance up to 500 episodes, giving no indication that the NFs lacks sufficient expressive power to be competitive.

Additionally, the graphs in Figure 1 reveal two apparent outliers for DP, namely *Beat Block Hammer* with 200 training episodes, and *Handover Block* with 100 training

episodes. While there may be other causes, we believe it is likely that these outliers result from high variance in the quality of the trained diffusion model. Overall, the performance of DP appears less stable and more unpredictable. In contrast, NF-P’s performance curve is generally more monotonic, consistently improving or leveling off, but rarely regressing, which potentially indicates a more stable training process. However, more data is required to make a definitive statement.

As seen in the table in Figure 1, NF-P consistently achieves higher success rates with fewer training episodes compared to DP. This is most evident in the *Lift Pot* task, where our NF-P variants respectively reach an 80% and 59% success rate with only 50 episodes, while DP only achieves 37% at the same point and requires 200 episodes to match NF-Ps performance. Similarly, in *Beat Block Hammer*, NF-P achieves a 40% and 29% success rate with 25 episodes, where DP’s performance is 16%. This superior sample efficiency demonstrates NF-P’s ability to learn robust

TABLE II

NF-P ABLATIONS. SUCCESS RATE FROM 100 TRIALS OF THE BEAT BLOCK HAMMER TASK. THE DEFAULT CONFIGURATION IS  $s = 4$ ,  $\sigma = 0.5$ , OPTIMIZED USING 10 STEPS OF GRADIENT ASCENT WITH ADAM (LEARN RATE=0.1).

Ablation	Result	
NF-P <sub>opt</sub>	$s = 4$	$\sigma = 0.5$
NF-P <sub>multi</sub>	$s = 4$	$\sigma = 0.5$
NF-P	$s = 4$	$\sigma = 0.5$
NF-P <sub>opt</sub>	$s = 8$	$\sigma = 0.5$
NF-P <sub>opt</sub>	$s = 2$	$\sigma = 0.5$
NF-P <sub>opt</sub>	$s = 1$	$\sigma = 0.5$
NF-P <sub>opt</sub>	$s = 4$	$\sigma = 1.0$
NF-P <sub>opt</sub>	$s = 4$	$\sigma = 0.75$
NF-P <sub>opt</sub>	$s = 4$	$\sigma = 0.25$
NF-P	No action sequencing	
	28	
	<b>51</b>	

policies from a smaller number of demonstrations, making it a highly practical choice for real-world applications where data collection is often costly and time-consuming.

Beyond performance and scaling, NF-P offers significant advantages in both architecture and inference speed. The simple feed-forward architecture of our NF-P allows it to be less resource-intensive and, perhaps most importantly, allows for an order of magnitude faster inference, as seen in Table I. While Diffusion Policy requires multiple sequential denoising steps to generate an action, Normalizing Flow Policy can perform inference in a single forward pass through the network, resulting in an inference time under 20ms. Fast action generation, in turn, is a crucial advantage for real-time robotics, where low latency is crucial for responsive and accurate control.

### B. Ablation Study

In this section, we conduct an ablation study in order to validate our design choices for NF-P. To verify the main factor of the performance, we include the following ablations:

- Different values for the time-domain stride  $s$  used when training (default:  $s = 4$ ).
- Different values for the sampling  $\sigma$  (default:  $\sigma = 0.5$ ).
- Different sampling strategies: NF-P<sub>opt</sub>, NF-P<sub>multi</sub>, and NF-P (no sample optimization).
- No action sequencing. In other words predicting only one action at a time.

1) *Result*: Table II shows the success rate on Task *Beat Block Hammer* as model parameters change. Each test was completed by a model trained on 50 episodes of training data. We also provide the default parameter settings used for our comparison with DP as a reference.

2) *Discussion*: First and foremost, we want to direct attention toward the fact that NF-P<sub>multi</sub> offers comparable performance to NF-P<sub>opt</sub>, as is also confirmed in Figure 1. This is noteworthy primarily because of the major difference in inference times between the two methods (recall Table I). As such, it appears that multi-sampling is a viable technique for achieving high performance even in scenarios where latency is critical.

Second, we note that removing action sequencing, and only predicting one action at a time, appears to drastically lower performance, thus validating the efficacy of predicting longer action sequences.

Finally, we observe that, with regards to both  $s$  and  $\sigma$ , the best performance is found with middle-ground values. We believe this confirms our initial hypotheses regarding these methods. To elaborate, we believe that the stride value  $s = 4$  provides a good tradeoff between large actions to reduce stalling, and small enough actions to avoid more erratic motions. Similarly, we believe that  $\sigma = 0.5$  offers a good tradeoff between exploring the state-space with larger actions, while avoiding the worst erratic motions. It is worth noting that  $\sigma$  in no way restricts the sample space, but only helps guide NF-P higher-probability samples.

## VI. CONCLUSIONS

In this work, we have demonstrated that Normalizing Flows Policy, a novel approach based on Normalizing Flows, provides a compelling alternative to Diffusion Policy for robotic manipulation tasks. Our findings show that NF-P consistently achieves superior or comparable performance across various tasks, particularly in data-sparse environments. Furthermore, the model’s training is presumably more stable and predictable compared to Diffusion Policy, and its single-pass inference provides a significant advantage in real-time applications with stricter latency requirements, making it a highly practical choice for robotic control.

## VII. FUTURE WORK

While we have explored several different techniques for making NFs viable and even competitive in the domain of visuomotor policy learning, our work is by no means exhaustive. One such method that we left unexplored is the addition of noise during training [18]. It would be an interesting direction to investigate how adding noise behaves in conjunction with out gradient ascent likelihood-optimization, since the noise removal is effectively equivalent to one step of gradient ascent. There are also works, for example [14], that attempt to improve inference times in diffusion models by updating an existing action sequence using fewer denoising steps compared to generating actions from scratch. Similar approaches could be explored for NFs. However, in the case of NFs, we believe such approaches would rather be applicable for improving consistency and smoothness in the action sequences, since the NF’s single-pass inference already provides low latency. Another potential research direction could be to evaluate different NFs architectures. In this work, we adopted coupling layers due to their fast inference and ability to directly evaluate their probability density. There are, however, other NFs architectures that have shown competitive performance in various generative tasks [24]. Finally, our previous research has shown how NFs can be used as a complement to improve the performance of other models by providing a robust measure of confidence [21], [22]. It is possible that NFs could be applied in conjunction

with for example DP or a transformer-based model to further improve performance.

## ACKNOWLEDGMENT

This research is funded by the Excellence Center at Linköping-Lund in Information Technology (ELLIIT), and the Wallenberg AI, Autonomous Systems and Software Program (WASP). We thank the computations enabled by the Berzelius resource provided by the Knut and Alice Wallenberg Foundation at the National Supercomputer Centre.

We thank Hashim Ismail for continued discussion and feedback.

## REFERENCES

- [1] C. Chi, Z. Xu, S. Feng, E. Cousineau, Y. Du, B. Burchfiel, R. Tedrake, and S. Song, "Diffusion policy: Visuomotor policy learning via action diffusion," *The International Journal of Robotics Research*, 2024.
- [2] J. Ho, A. Jain, and P. Abbeel, "Denoising diffusion probabilistic models," *arXiv preprint arXiv:2006.11239*, 2020.
- [3] G. Papamakarios, E. Nalisnick, D. J. Rezende, S. Mohamed, and B. Lakshminarayanan, "Normalizing flows for probabilistic modeling and inference," *Journal of Machine Learning Research*, vol. 22, no. 57, pp. 1–64, 2021. [Online]. Available: <http://jmlr.org/papers/v22/19-1028.html>
- [4] T. Chen, Z. Chen, B. Chen, Z. Cai, Y. Liu, Q. Liang, Z. Li, X. Lin, Y. Ge, Z. Gu, *et al.*, "Robotwin 2.0: A scalable data generator and benchmark with strong domain randomization for robust bimanual robotic manipulation," *arXiv preprint arXiv:2506.18088*, 2025.
- [5] Z. Gong, P. Ding, S. Lyu, S. Huang, M. Sun, W. Zhao, Z. Fan, and D. Wang, "Carp: Visuomotor policy learning via coarse-to-fine autoregressive prediction," *arXiv preprint arXiv:2412.06782*, 2024.
- [6] A. Brohan, N. Brown, J. Carbalajal, Y. Chebotar, J. Dabis, C. Finn, K. Gopalakrishnan, K. Hausman, A. Herzog, J. Hsu, *et al.*, "Rt-1: Robotics transformer for real-world control at scale," *arXiv preprint arXiv:2212.06817*, 2022.
- [7] S. Lee, Y. Wang, H. Etukuru, H. J. Kim, N. M. M. Shafullah, and L. Pinto, "Behavior generation with latent actions," *arXiv preprint arXiv:2403.03181*, 2024.
- [8] S. Haldar, Z. Peng, and L. Pinto, "Baku: An efficient transformer for multi-task policy learning, 2024," URL <https://arxiv.org/abs/2406.07539>.
- [9] P. Florence, C. Lynch, A. Zeng, O. A. Ramirez, A. Wahid, L. Downs, A. Wong, J. Lee, I. Mordatch, and J. Tompson, "Implicit behavioral cloning," in *Conference on robot learning*. PMLR, 2022, pp. 158–168.
- [10] X. Ma, S. Patidar, I. Haughton, and S. James, "Hierarchical diffusion policy for kinematics-aware multi-task robotic manipulation," in *Proceedings of the IEEE/CVF Conference on Computer Vision and Pattern Recognition*, 2024, pp. 18 081–18 090.
- [11] J. Ma, Y. Qin, Y. Li, X. Liao, Y. Guo, and R. Zhang, "Cdp: Towards robust autoregressive visuomotor policy learning via causal diffusion," *arXiv preprint arXiv:2506.14769*, 2025.
- [12] Z. Wang, Z. Li, A. Mandlekar, Z. Xu, J. Fan, Y. Narang, L. Fan, Y. Zhu, Y. Balaji, M. Zhou, *et al.*, "One-step diffusion policy: Fast visuomotor policies via diffusion distillation," *arXiv preprint arXiv:2410.21257*, 2024.
- [13] Y. Ze, G. Zhang, K. Zhang, C. Hu, M. Wang, and H. Xu, "3d diffusion policy: Generalizable visuomotor policy learning via simple 3d representations," *arXiv preprint arXiv:2403.03954*, 2024.
- [14] Y. Duan, H. Yin, and D. Kragic, "Real-time iteration scheme for diffusion policy," *arXiv preprint arXiv:2508.05396*, 2025.
- [15] K. Black, N. Brown, D. Driess, A. Esmail, M. Equi, C. Finn, N. Fusai, L. Groom, K. Hausman, B. Ichter, S. Jakubczak, T. Jones, L. Ke, S. Levine, A. Li-Bell, M. Mothukuri, S. Nair, K. Pertsch, L. X. Shi, J. Tanner, Q. Vuong, A. Walling, H. Wang, and U. Zhilinsky, " $\pi_0$ : A vision-language-action flow model for general robot control," 2024. [Online]. Available: <https://arxiv.org/abs/2410.24164>
- [16] K. Black, N. Brown, J. Darpinian, K. Dhabalia, D. Driess, A. Esmail, M. Equi, C. Finn, N. Fusai, M. Y. Galliker, *et al.*, " $\pi_0$ . 5: a vision-language-action model with open-world generalization," *arXiv preprint arXiv:2504.16054*, 2025.
- [17] L. Dinh, J. Sohl-Dickstein, and S. Bengio, "Density estimation using real nvp," 2017. [Online]. Available: <https://arxiv.org/abs/1605.08803>
- [18] S. Zhai, R. Zhang, P. Nakkiran, D. Berthelot, J. Gu, H. Zheng, T. Chen, M. A. Bautista, N. Jaitly, and J. Susskind, "Normalizing flows are capable generative models," *arXiv preprint arXiv:2412.06329*, 2024.
- [19] R. Ghugare and B. Eysenbach, "Normalizing flows are capable models for rl," *arXiv preprint arXiv:2505.23527*, 2025.
- [20] D. P. Kingma and P. Dhariwal, "Glow: Generative flow with invertible 1x1 convolutions," 2018. [Online]. Available: <https://arxiv.org/abs/1807.03039>
- [21] S. Kristoffersson Lind, R. Triebel, L. Nardi, and V. Krueger, "Out-of-distribution detection for adaptive computer vision," in *Image Analysis*, ser. Lecture Notes in Computer Science, R. Gade, M. Felsberg, and J.-K. Kämäriäinen, Eds. Cham: Springer Nature Switzerland, 2023, p. 311–325.
- [22] S. K. Lind, R. Triebel, and V. Krüger, "Making the flow glow – robot perception under severe lighting conditions using normalizing flow gradients," no. arXiv:2412.07565, Dec. 2024, arXiv:2412.07565 [cs]. [Online]. Available: <http://arxiv.org/abs/2412.07565>
- [23] J. Song, C. Meng, and S. Ermon, "Denoising diffusion implicit models," *arXiv:2010.02502*, October 2020. [Online]. Available: <https://arxiv.org/abs/2010.02502>
- [24] C. Durkan, A. Bekasov, I. Murray, and G. Papamakarios, *Neural spline flows*. Red Hook, NY, USA: Curran Associates Inc., 2019.
- [25] K. He, X. Zhang, S. Ren, and J. Sun, "Deep residual learning for image recognition," 2015. [Online]. Available: <https://arxiv.org/abs/1512.03385>
- [26] D. P. Kingma and J. Ba, "Adam: A method for stochastic optimization," 2017. [Online]. Available: <https://arxiv.org/abs/1412.6980>
- [27] H. Yu, Y. Jin, Y. He, and W. Sui, "Efficient task-specific conditional diffusion policies: Shortcut model acceleration and so (3) optimization," in *Proceedings of the Computer Vision and Pattern Recognition Conference*, 2025, pp. 4174–4183.
- [28] G. Yan, J. Zhu, Y. Deng, S. Yang, R.-Z. Qiu, X. Cheng, M. Memmel, R. Krishna, A. Goyal, X. Wang, *et al.*, "Maniflow: A general robot manipulation policy via consistency flow training," *arXiv preprint arXiv:2509.01819*, 2025.
- [29] D. Huang, Z. Cai, Y. Hao, Z. Li, and C.-M. Chew, "Prism: Point-cloud reintegrated inference via segmentation and cross-attention for manipulation," *IEEE Robotics and Automation Letters*, 2025.